

Structure and Charge Control in Metal–Organic Frameworks Based on the Tetrahedral Ligand Tetrakis(4-tetrazolylphenyl)methane

Mircea Dincă,^[a] Anne Dailly,^[b] and Jeffrey R. Long^{*[a]}

Abstract: Use of the tetrahedral ligand tetrakis(4-tetrazolylphenyl)methane enabled isolation of two three-dimensional metal–organic frameworks featuring 4,6- and 4,8-connected nets related to the structures of garnet and fluorite with the formulae $\text{Mn}_6(\text{ttpm})_3 \cdot 5\text{DMF} \cdot 3\text{H}_2\text{O}$ (**1**) and $\text{Cu}_4[(\text{Cu}_4\text{Cl})(\text{ttpm})_2]_2 \cdot \text{CuCl}_2 \cdot 5\text{DMF} \cdot 11\text{H}_2\text{O}$

(**2**) (H_4ttpm = tetrakis(4-tetrazolylphenyl)methane). The fluorite-type solid **2** displays an unprecedented post-synthetic transformation in which the neg-

Keywords: copper • manganese • metal–organic frameworks • microporous materials • tetrazoles

ative charge of the framework is reduced by extraction of copper(II) chloride. Desolvation of this compound generates $\text{Cu}_4(\text{ttpm})_2 \cdot 0.7\text{CuCl}_2$ (**2d**), a microporous material exhibiting a high surface area and significant hydrogen uptake.

Introduction

Owing to their porosity and potential utility in a wide variety of applications, especially in gas storage, separations, and catalysis, metal–organic frameworks have attracted considerable recent attention. In particular, reports of frameworks with surface areas well above those of any zeolites,^[1] with high hydrogen-storage capacities,^[2] or displaying unprecedented gas separation or catalytic properties^[3] have strengthened the wide-spread interest in the field. To construct materials with such remarkable properties, researchers must rely on somewhat serendipitous synthetic methods, which more often than not produce materials with no permanent porosity. Although it is not generally possible to predict the stability of a given framework upon guest evacuation, empirical observations show that the vast majority of permanently porous frameworks covalently extend in three dimensions.^[4] Surprisingly, however, most known three-di-

mensional frameworks are based on planar, aromatic bridging ligands that need not assemble into three-dimensional structures. Instead, three-dimensionality in these frameworks is enforced by the metal building units, which usually consist of multinuclear clusters synthesized in situ from single metal-ion precursors.^[5] Although mathematical and computational principles have been laid out to understand and sometimes predict the topology of frameworks based on certain cluster building units,^[6] the synthetic conditions required to target a given cluster are still poorly understood. As such, the synthesis of three-dimensional frameworks starting from simple, two-dimensional ligands remains largely a matter of trial and error.

A potentially more efficient way to synthesize three-dimensional metal–organic frameworks is to focus on the organic ligands rather than the metal building unit, and to utilize one of the many readily available three-dimensional organic scaffolds, such as tetraphenylmethane, adamantane, or spirane. Indeed, employing a three-dimensional bridging ligand promotes the formation of a three-dimensional framework, regardless of the geometry around the metal building unit. Herein, we show that use of the tetrahedral molecule tetrakis(4-tetrazolylphenyl)methane (H_4ttpm) leads to the formation of two new three-dimensional frameworks with rare 4,6- and 4,8-connected topologies identical to those of garnet (*gar*) and fluorite (*flu*).^[6d] We further show that solvent exchange in the *flu*-type framework coincides with an anionic-to-neutral post-synthetic transformation that has not been observed in metal–organic frameworks thus far, and that evacuation of this framework pro-

[a] M. Dincă, Prof. J. R. Long
Department of Chemistry
University of California at Berkeley
Berkeley CA, 94720-1460 (USA)
Fax: (+1) 510-643-3546
E-mail: jrlong@berkeley.edu

[b] Dr. A. Dailly
Chemical and Environmental Sciences Laboratory
General Motors Corporation
Warren MI, 48090 (USA)

Supporting information for this article is available on the WWW under <http://dx.doi.org/10.1002/chem.200801336>.

duces a material with permanent porosity and high surface area.

Results and Discussion

The tetrahedral ligand H_4ttpm was synthesized by a dipolar [2+3] cycloaddition between NaN_3 and tetra(*p*-cyanophenyl)methane, which in turn was obtained from tetraphenylmethane via tetra(*p*-bromophenyl)methane.^[7] To explore the ability of H_4ttpm to promote the formation of porous three-dimensional metal–organic frameworks, we screened synthetic conditions that had previously been effective in the formation of transition-metal–tetrazolate frameworks. Thus, solventothermal reactions between H_4ttpm and $Mn(NO_3)_2 \cdot 4H_2O$ or $CuCl_2 \cdot 2.5H_2O$ in mixtures of DMF and methanol produced colorless or green crystals of $Mn_6(ttpm)_3 \cdot 5DMF \cdot 3H_2O$ (**1**) or $Cu[(Cu_4Cl)(ttpm)_2]_2 \cdot CuCl_2 \cdot 5DMF \cdot 11H_2O$ (**2**), respectively.

X-ray analysis of a single crystal of **1** revealed a structure in which linear Mn_3 clusters are connected to six distinct $ttpm^{4-}$ ligands to form a neutral three-dimensional framework (Figure 1). Here, each trimetallic unit consists of a central Mn^{2+} ion octahedrally coordinated by nitrogen atoms from six tetrazolate rings, and two outer Mn^{2+} ions, each bridged to the central Mn^{2+} ion by three tetrazolate rings and facially coordinated by three solvent molecules.^[8] Overall, each trinuclear unit is surrounded by six tetrazolate rings and can thus be described as a six-connected node. Although such linear trimetallic units are common in both tetrazolate- and carboxylate-based frameworks,^[9] their unique combination here with the four-connected nodes corresponding to the $ttpm^{4-}$ ligands gives rise to a rare 4,6-connected framework with the garnet topology (*gar*). Notably, this highly-connected topology has, to our knowledge, only been observed once before in a metal–organic framework: in the structure of $In_3Zn_2(im)_{12}$ ($im^- = imidazolate$).^[10]

X-ray analysis of a single crystal of **2** revealed a structure in which chloride-centered,

square-planar $\{Cu_4Cl\}^{7+}$ units are bridged by eight distinct $ttpm^{4-}$ ligands to form a three-dimensional structure (Figure 2). Within a given $\{Cu_4Cl\}^{7+}$ unit, each Cu^{2+} ion is coordinated by four nitrogen atoms and one chloride anion, whereas pairs of neighboring Cu^{2+} ions are bridged by two tetrazolate rings, such that overall, the cluster can be described as an eight-connected node. The resulting net anionic charge of the framework in **2** is balanced by extraframework Cu^{2+} ions, which are chelated by two nitrogen atoms on adjacent tetrazolate rings. Notably, X-ray analysis also revealed that the structure of **2** includes one full equivalent of $CuCl_2$, such that the sixth coordination site on the intraframework Cu^{2+} cations is occupied by a solvent molecule 75 % of the time and by a chloride anion 25 % of the time.

Although square-planar clusters surrounded by eight bridging ligands have been observed previously in the structures of Mn- and Cu-tetrazolate frameworks,^[2d,11] and in Fe-, Co-, and Cd-based carboxylate frameworks,^[12] their combination here with the tetrahedral four-connected nodes corre-

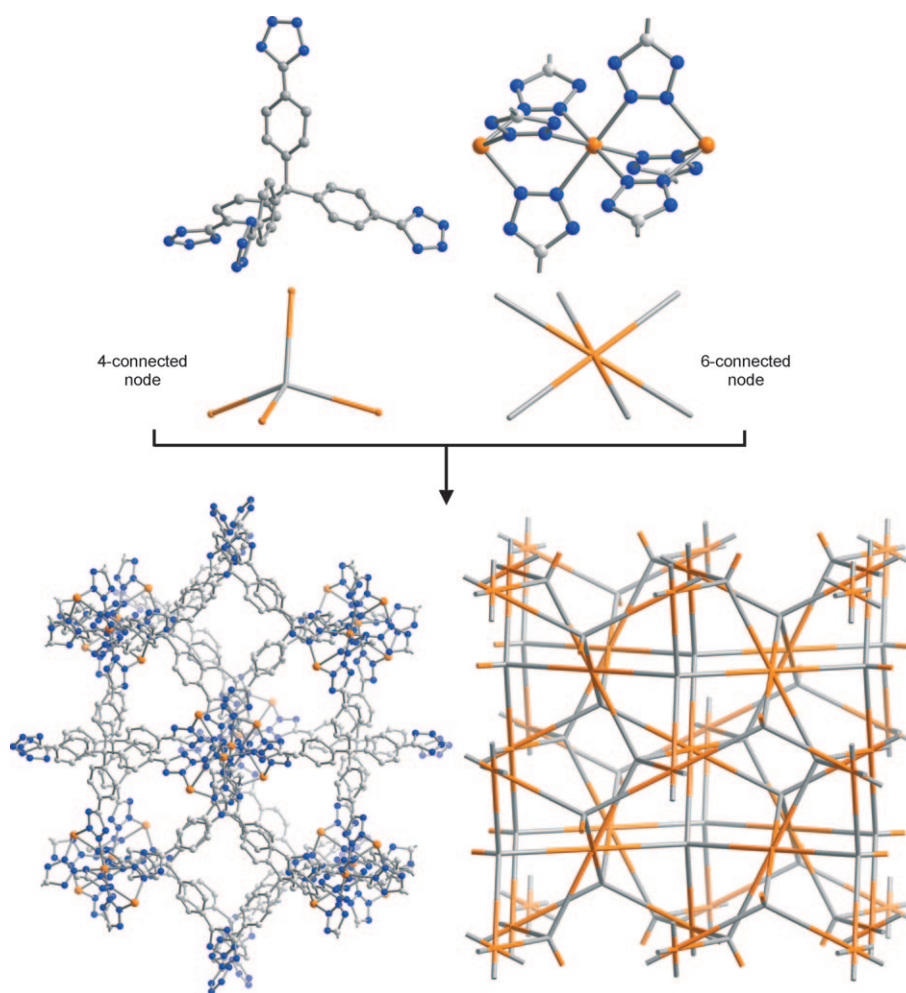


Figure 1. Portions of the crystal structure of **1**: the four- and six-connected nodes, depicted in grey and orange and representing $ttpm^{4-}$ and $[Mn_3(tetrazolate)_6]$ units, respectively, combine to form a three-dimensional structure with the garnet topology. Orange, grey, and blue spheres represent Mn, C, and N atoms, respectively; solvent molecules and hydrogen atoms are omitted for clarity. Selected interatomic distances [Å] and angles [°]: $Mn_{central}-N$ 2.32(2), $Mn_{exterior}-N$ 2.25(2), $Mn_{exterior}-O$ 2.16(1), $Mn \cdots Mn$ 4.05(3); $N-Mn-N$ 87(1), $Mn-N-N$ 127(1).

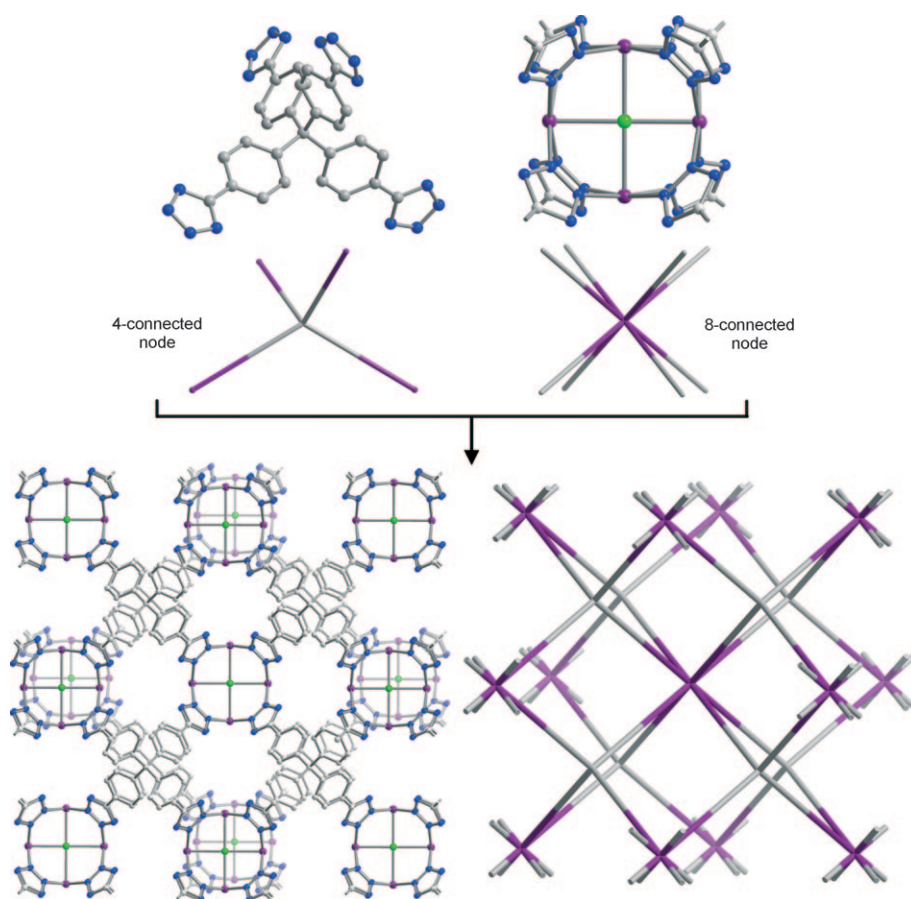


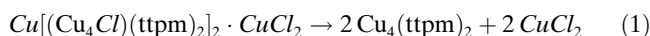
Figure 2. Portions of the crystal structure of **2**: the four- and eight-connected nodes, depicted in grey and purple and represented by ttpm^{4-} and $[\text{Cu}_4\text{Cl}(\text{tetrazolate})_8]$ units, respectively, combine to form a three-dimensional structure with the fluorite topology. Purple, green, blue, and grey spheres represent Cu, Cl, N, and C atoms, respectively. Solvent molecules and hydrogen atoms were omitted for clarity. Selected interatomic distances [Å] and angles [°]: Cu–Cl 2.539(1), Cu–N 2.036(3), Cu⋯Cu 3.590(1); Cu–Cl–Cu 90, N–Cu–N 87.25(1), 92.23(1), Cu–N–N 123.88(1).

sponding to the ttpm^{4-} ligands gives rise to another rare net—a 4,8-connected net with the fluorite topology (*flu*). Notably, the structure of **2** is isotypic with that of $\text{Cd}_2(\text{tcpm})$ ^[12a] (H_4tcpm = tetra(*p*-carboxyphenyl)methane), one of only two other examples of metal–organic frameworks exhibiting the *flu* topology.^[13]

Space-filling diagrams of the structures of **1** and **2** suggested that evacuation of the guest and bound solvent molecules could potentially give rise to microporous solids in both cases. To test the porosity of the two materials, as-synthesized samples were first soaked in distilled methanol to exchange high-boiling DMF from within the pores with a lower-boiling solvent. We have previously shown that this technique allows evacuation of a given framework at a reduced temperature, thus diminishing the possibility of collapse upon guest removal.^[2d] Despite this precautionary step, desolvated samples of **1** did not retain crystallinity and showed no significant gas uptake, suggesting that framework collapse in this case occurs even under relatively mild evacuation conditions. Indeed, although previous examples of tetrazolate-bridged frameworks based on linear trimetallic

units showed comparatively higher porosity, samples of $\text{Mn}_3(\text{bdt})_3$ and $\text{Zn}_3(\text{bdt})_3$ (bdt^{2-} = 1,4-benzenedithiazolate) also had a high propensity for collapse upon solvent evacuation.^[9e]

Unlike **1**, crystals of as-synthesized **2** remained intact both during methanol exchange and, more importantly, upon evacuation at 65 °C under reduced pressure. The behavior of **2** towards solvent exchange and guest evacuation is similar to that observed previously for $\text{Mn}_3[(\text{Mn}_4\text{Cl})_3(\text{btt})_8(\text{CH}_3\text{OH})_{10}]_2$ and $\text{H}_2\text{Cu}[(\text{Cu}_4\text{Cl})_3(\text{btt})_8]\cdot 3.5\text{HCl}$ (btt^{3-} = 1,3,5-benzenetristetrazolate),^[2d,11a] two related frameworks containing analogous square-planar $[\text{M}_4\text{Cl}]^{7+}$ building units. In stark contrast to the btt^{3-} -based structures, however, initial X-ray analysis of an evacuated crystal of **2** revealed a surprisingly low occupancy of the central Cl^- anion. This suggests that methanol exchange could in principle extract CuCl_2 equivalents from **2** to provide a neutral framework with the formula $\text{Cu}_4(\text{ttpm})_2$, which would be composed entirely of chloride-voided Cu_4 squares, as described by Equation (1):



The prospect of effecting an anionic-to-neutral transformation is particularly attractive in **2** because the chloride-deficient Cu_4 squares that would be formed upon extraction of CuCl_2 could potentially serve as strong binding pockets for small molecules, such as O_2 , N_2 , or H_2 . In an effort to probe the possibility of such a transformation, we employed a strategy involving a Soxhlet extraction of CuCl_2 from a fresh sample of **2** with hot methanol. The initially colorless solvent gradually turned green, confirming the extraction of CuCl_2 from the crystals of **2**. After five days, methanol-washed single crystals of **2** were collected by filtration and evacuated at 65 °C under reduced pressure to produce $\text{Cu}_4(\text{ttpm})_2\cdot 0.7\text{CuCl}_2$ (**2d**). As expected, X-ray analysis of an evacuated single crystal of **2d** revealed a further decrease of the Cl^- occupancy at the central position within the square-planar $[\text{Cu}_4\text{Cl}]^{7+}$ units. Although partially occupied Cl^- anions are still bound to outside axial positions of Cu_4 units in **2d**, X-ray analysis suggested that the Soxhlet extraction

eliminated the central Cl^- anion from ca. 50% of the $\{\text{Cu}_4\text{Cl}\}^{7+}$ clusters. Despite the fact that only a limited amount of CuCl_2 was eliminated from **2** under these conditions, the transformation from **2** to **2d** represents the first example of a postsynthetic modification in which the charge of the metal–organic framework is reduced.

Further evidence of CuCl_2 elimination from **2** comes, as one may expect, from the significant structural changes caused by the loss of Cl^- from the square-planar $\{\text{Cu}_4\text{Cl}\}^{7+}$ building units. In this context, the most significant changes were observed in the length of the Cu–N bonds and the *trans* Cu...Cu distances, which were shortened from 2.036(3) and 5.078(2) Å, respectively, in **2**, to 1.985(3) and 4.932(2) Å, respectively, in **2d**. However, despite a shortening of the distances within the square-planar units, which are situated parallel to the *ac* plane, the *a* and *c* parameters are in fact larger in **2d** than in **2**, as shown in Table 1. This seemingly counterintuitive observation is due to a reorganization of the tetrahedral ligand, wherein the acute angle between two of the arms widens from 84(1) in **2** to 89(1)° in **2d**.

Table 1. Comparison of the tetragonal unit-cell dimensions for **2** and **2d**.

	2	2d	Difference ([%])
<i>a</i> [Å]	15.501	16.091	0.59 (3.8)
<i>c</i> [Å]	29.401	28.187	−1.214 (−4.1)
<i>V</i> [Å ³]	7064	7299	235 (3.3)

As such, the *a* and *c* cell edges are extended, whereas the *b* parameter is shortened for an overall cell volume augmentation of 3.3% in going from **2** to **2d**. In **2d**, two types of pores exist: tetragonally-distorted octahedral cage-like pores defined by six $\{\text{Cu}_4\text{Cl}\}^{7+}$ units and eight ttpm^{4-} ligands and with interior atom-to-atom dimensions of $27.5 \times 17.8 \times 17.8$ Å³, and rhombohedral-shaped two-dimensional channels running parallel to the *ac* plane, with diagonal atom-to-atom dimensions of 14.1×12.6 Å².

An N_2 adsorption isotherm for **2d**, shown in Figure 3, revealed a reversible Type I adsorption isotherm with a saturat-

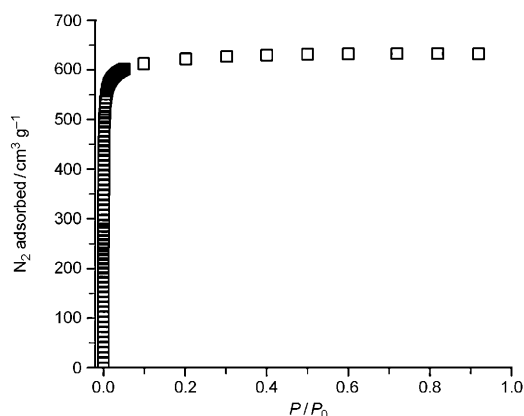


Figure 3. Isotherm for the adsorption of N_2 within **2d** at 77 K.

tion amount of $640 \text{ cm}^3 \text{ g}^{-1}$ at 1 bar. Fits of the isotherm employing the BET and Langmuir models gave apparent surface areas of 2506(2) and 2745(3) $\text{m}^2 \text{ g}^{-1}$, respectively. Significantly, these represent the highest surface areas yet reported for a tetrazolate-bridged framework, surpassing the previous record held by $\text{Ni}_{2.75}\text{Mn}_{0.25}[(\text{Mn}_4\text{Cl})_3(\text{btt})_8]_2 \cdot 20 \text{ CH}_3\text{OH}$, which exhibits a BET surface area of 2110(5) $\text{m}^2 \text{ g}^{-1}$ and a Langmuir surface area of 2282(8) $\text{m}^2 \text{ g}^{-1}$.^[14]

The combination of high internal surface area and exposed metal coordination sites suggested that compound **2d** might be of interest for hydrogen storage applications. Indeed, its H_2 adsorption isotherm at 77 K revealed a reversible uptake of 2.8 wt % at 1.2 bar (Figure 4), representing

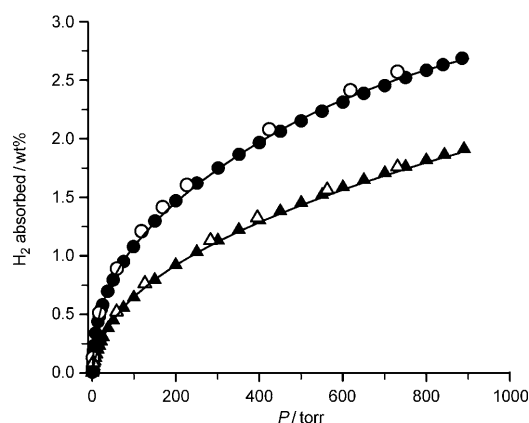


Figure 4. Isotherms for the excess uptake of H_2 within **2d** at 77 K (●, ○) and at 87 K (▲, △). Filled and empty symbols represent adsorption and desorption data, respectively, whereas the lines correspond to the virial fits to the two adsorption isotherms.

one of the highest H_2 uptakes reported for a metal–organic framework under these conditions.^[15] Measurement of an H_2 adsorption isotherm at 87 K and fitting of the combined 77 and 87 K isotherms allowed calculation of the isosteric heat of adsorption, which showed a zero-coverage value of 8.4 kJ mol^{-1} . This is slightly lower than the value of 9.4 kJ mol^{-1} established for $\text{HCu}[(\text{Cu}_4\text{Cl})_3(\text{btt})_8] \cdot 3.5 \text{ HCl}$.^[11a] The lower zero-coverage enthalpy of adsorption in **2d** is likely a consequence of the reduction in the number of strong H_2 binding sites due to the presence of Cl^- anions and the fact that, as evidenced by X-ray crystallography, only 70% of the Cu^{2+} sites are available for H_2 binding, with Cl^- anions occupying the rest of the available sites. Further H_2 adsorption measurements at pressures up to 70 bar revealed an excess H_2 uptake of 4.1 wt % at 20 bar and 77 K, as shown in Figure 5. The total uptake of 5.6 wt % at 70 bar (corresponding to a volumetric H_2 storage density of 41 g L^{-1}), is comparable to the total gravimetric uptakes of $\text{Mn}_3[(\text{Mn}_4\text{Cl})_3(\text{btt})_8(\text{CH}_3\text{OH})_{10}]_2$ and $\text{HCu}[(\text{Cu}_4\text{Cl})_3(\text{btt})_8] \cdot 3.5 \text{ HCl}$,^[2d, 11] which at 70 bar showed total uptakes of 6.7 and 5.6 wt %, respectively, but is lower than the total H_2

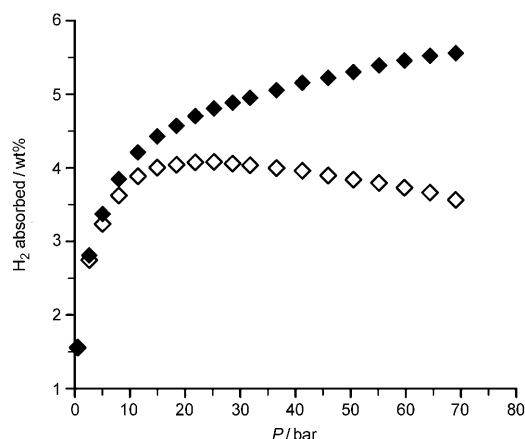


Figure 5. Isotherms for the adsorption of H_2 within **2d** at 77 K. Empty and solid symbols represent excess and total uptake, respectively.

uptake of 9.4 wt % observed for $Zn_4O(1,4\text{-benzenedicarboxylate})_3$ under these conditions.^[2g]

Conclusion

The foregoing results show that use of predesigned three-dimensional organic ligands can circumvent the formation of low-dimensional systems, enabling isolation of metal–organic frameworks with rare, highly-connected three-dimensional topologies. Herein, two contrasting examples serve to reiterate that predicting the stability of any given framework to desolvation remains a great challenge, but that targeting three-dimensional systems by using this strategy can be an effective way for discovering new materials with permanent porosity. Future efforts will focus on further developing the coordination chemistry of three-dimensional bridging ligands such as $H_4\text{ttpm}$ and its adamantane-centered analogue. In addition, the unprecedented capability of the $\{Cu_4Cl\}^{7+}$ tetrazolate clusters to eliminate chloride anions will be explored in the context of sequestering small molecules for potential applications in their storage, activation, and catalytic transformation.

Experimental Section

General: All reagents were obtained from commercial vendors and, unless otherwise noted, were used without further purification. Methanol was distilled over Mg/I_2 prior to use. The compound tetra(*p*-cyanophenyl)methane was synthesized according to a previously published procedure.^[7] **Caution!** Although we did not encounter any incident while handling the compounds described herein, metal azides and tetrazoles are potentially explosive and should be handled with great care.

Tetrakis(4-2H-tetrazol-5-yl-phenyl)methane heptahydrate ($H_4\text{ttpm}\cdot 7H_2O$): A mixture of tetra(*p*-cyanophenyl)methane (0.62 g, 1.5 mmol), NaN_3 (1.2 g, 18 mmol), and triethylamine hydrochloride (2.5 g, 18 mmol) in toluene (25 mL) and methanol (5 mL) was heated at reflux in a 100 mL round-bottomed flask for 4 d. Upon cooling to room temperature, an aqueous solution of NaOH (25 mL, 1 M) was added, and the mixture was stirred for 30 min. The aqueous layer was treated with

dilute HCl (ca. 50 mL, 1 M) until no further precipitate formed. The precipitate was then collected by filtration, dried in air, and dissolved in aqueous NaOH (1 M). The resulting clear, colorless solution was titrated with dilute HCl (ca. 20 mL, 1 M) until the pH of the solution was 4. The ensuing precipitate was washed with distilled water (3×150 mL) and dried in air to afford 0.75 g (70 %) of product as a white powder. 1H NMR ($[D_6]DMSO$, 400 MHz): δ = 8.05 (d, 8 H, J = 8.8 Hz), 7.57 ppm (d, 8 H, J = 8.8 Hz); ^{13}C NMR ($D_6]DMSO$, 400 MHz): δ = 131.7, 127.4 ppm (aromatic tertiary C); IR (neat): $\tilde{\nu}$ = 3364 (m, br), 3215 (m, br), 3105 (m, br), 3033 (m, br), 2941 (w, br), 2876 (m, br), 2775 (m, br), 1614 (s), 1568 (s), 1501 (vs), 1439 (s), 1250 (m), 1155 (m), 1074 (m), 1025 (w), 998 (m), 760 (m), 748 (s), 733 (s), 704 cm^{-1} (s); elemental analysis calcd (%) for $C_{25}H_{20}N_{16}\cdot 7H_2O$: C 48.46, H 4.77, N 31.18; found: C 48.66, H 4.78, N 31.13.

$Mn_6(\text{ttpm})_3\cdot 5DMF\cdot 3H_2O$ (1): Solid $Mn(NO_3)_2\cdot 4H_2O$ (190 mg, 0.95 mmol) and $H_4\text{ttpm}\cdot 7H_2O$ (50 mg, 0.070 mmol) were dissolved in a mixture of DMF (10 mL) and methanol (8 mL) inside a 20 mL scintillation vial sealed with a Teflon-lined cap. The vial was heated at 75 °C for 4 d. Colorless cube-shaped crystals deposited on the walls of the vial after ca. 2 d. The crystals were collected by filtration inside a nitrogen-filled glove bag, quickly rinsed with 10 mL of anhydrous DMF, and then soaked in distilled methanol. Upon evacuation at 85 °C, 40 mg (70 %) of product was obtained. IR (neat): $\tilde{\nu}$ = 3162 (br, m), 2828 (m), 1616 (w), 1450 (s), 1423 (m), 1230 (w), 1119 (w), 1003 (vs), 833 (vs), 763 (s), 735 (s), 647 cm^{-1} (vs); elemental analysis calcd (%) for $C_{102}H_{89}Mn_6N_{53}O_8$: C 48.71, H 3.58, N 29.52; found: C 46.90, H 2.85, N 29.23; this compound is water- and moisture-sensitive.

$Cu[(Cu_4Cl)(\text{ttpm})_2]_2\cdot CuCl_2\cdot 5DMF\cdot 11H_2O$ (2): Solid $CuCl_2\cdot 2H_2O$ (100 mg, 0.59 mmol) and $H_4\text{ttpm}\cdot 7H_2O$ (50 mg, 0.070 mmol) were dissolved in a mixture of DMF (7 mL) and methanol (3 mL) inside a 20 mL scintillation vial sealed with a Teflon-lined cap. The initially green suspension dissolved upon addition of concentrated HCl (ca. 20 μ L) to afford a clear bright-green solution, which was left undisturbed at room temperature for 4 d. Green tetragonal rodlike crystals were deposited on the bottom and walls of the vial, and were collected by filtration inside a nitrogen-filled glove bag and quickly rinsed with anhydrous DMF (10 mL). After drying at 75 °C under reduced pressure, a yield of 39 mg (61 %) of product was isolated. IR (neat): $\tilde{\nu}$ = 3035 (br, w), 1646 (s), 1607 (m), 1454 (vs), 1418 (m), 1369 (w), 1116 (w), 1062 (w), 1009 (m), 829 (vs), 759 (s), 739 (s), 695 cm^{-1} (m); elemental analysis calcd (%) for $C_{131}H_{121}Cl_4Cu_{10}N_{69}O_{16}$: C 42.58, H 3.30, N 26.16; found: C 42.66, H 2.88, N 25.96; this compound is sparingly soluble in DMF, insoluble in nonpolar organic solvents, and is water- and moisture-sensitive.

$Cu(\text{ttpm})_2\cdot 0.7CuCl_2$ (2d): A freshly-prepared sample of **2** was loaded into a Soxhlet extractor equipped with a water condenser. Freshly distilled methanol was heated to reflux and cycled through the sample for 5 d, during which it changed color to green. The methanol-washed crystals were then dried by heating at 65 °C under high vacuum ($<10^{-5}$ torr) for 2 d. IR (neat): $\tilde{\nu}$ = 3382 (br, w), 1614 (m), 1453 (vs), 1258 (w), 1162 (w), 1124 (w), 1072 (w), 1008 (s), 836 (s), 758 (m), 739 (m), 697 (w), 656 cm^{-1} (w); elemental analysis calcd (%) for $C_{38}H_{32}Cl_{1.4}Cu_{4.7}N_{32}\cdot 5.5H_2O$: C 42.88, H 2.67, N 27.59; found: C 43.04, H 2.25, N 27.19.

Gas adsorption measurements: Gas adsorption isotherms for pressures in the range 0–1.2 bar were measured by using a Micromeritics ASAP2020 instrument. High pressure H_2 adsorption isotherms were measured on a HyEnergy PCTPro-2000 instrument in a manner that has been previously described.^[2d] Ultra-high purity He (UHP grade 5.0, 99.999 % purity) was used for free-space measurements. H_2 and N_2 isotherms at 77 K were measured in liquid nitrogen baths by using UHP-grade gas sources. H_2 isotherms at 87 K were measured in liquid argon baths. Oil-free vacuum pumps and oil-free pressure regulators were used for all measurements to prevent contamination of the samples during the evacuation process, or of the feed gases during the isotherm measurement. The total amount of hydrogen stored in **2d** was calculated as previously described.^[2d]

X-ray structure determinations (see Table S1 in the Supporting Information): Crystals of **1**, **2**, and **2d** were coated in Paratone-N oil, attached to Kapton loops, transferred to a Siemens SMART APEX diffractometer,

and cooled in a dinitrogen stream. Lattice parameters were initially determined from a least-squares analysis of more than 100 centered reflections; these parameters were later refined against all data. None of the crystals showed significant decay during data collection. The raw intensity data were converted (including corrections for background, Lorentz, and polarization effects) to structure factor amplitudes and their esd's by using the SAINT 7.07b program. An empirical absorption correction was applied to each data set by using SADABS. Space-group assignment was based on systematic absences, *E*-statistics, and successful refinement of the structures. Structures were solved by direct methods with the aid of difference Fourier maps and were refined against all data by using the SHELXTL 5.0 software package. Hydrogen atoms were inserted at idealized positions and refined by using a riding model with an isotropic thermal parameter 1.2 times that of the attached carbon atom. To determine the correct stoichiometry for **2** and **2d**, the occupancies and thermal parameters of extraframework Cu and Cl atoms were refined freely. The disorder evidenced in the electron-density map prevented the refinement of solvent molecules within the pores of these three compounds. As such, all peaks with electron densities larger than one electron were refined as partially occupied oxygen and carbon atoms. The poor quality of the diffraction data and extreme disorder of the bound and guest solvent molecules led to relatively large R_1 and wR_2 values for the structure of **1**. However, the connectivity and structure of the skeleton within **1** was unequivocally determined by using this dataset. CCDC-690344, -690345, and -690346 contain the supplementary crystallographic data for this paper. These data can be obtained free of charge from The Cambridge Crystallographic Data Centre via www.ccdc.cam.ac.uk/data_request/cif.

Other physical measurements: IR spectra were collected on a Nicolet Avatar 360 FTIR spectrometer with an attenuated total reflectance accessory. ^1H NMR spectra were obtained by using a Bruker AVQ-400 instrument. Carbon, hydrogen, and nitrogen atom analyses were obtained from the Microanalytical Laboratory of the University of California, Berkeley. Powder X-ray diffraction patterns were recorded by using $\text{Cu}_{\text{K}\alpha}$ radiation ($\lambda = 1.5406 \text{ \AA}$) on a Bruker D8 Advance diffractometer.

Acknowledgements

This research was supported by the General Motors Corporation. We thank Dr. F. J. Hollander for assistance with solving the X-ray crystal structure of **1**.

- [1] a) H. K. Chae, D. Y. Siberio-Pérez, J. Kim, Y. Go, M. Eddaoudi, A. J. Matzger, M. O'Keeffe, O. M. Yaghi, *Nature* **2004**, *427*, 523; b) G. Férey, C. Mellot-Draznieks, C. Serre, F. Millange, J. Dutour, S. Surblé, I. Margiolaki, *Science* **2005**, *309*, 2040; c) D. Sun, S. Ma, Y. Ke, J. D. Collins, H.-C. Zhou, *J. Am. Chem. Soc.* **2006**, *128*, 3896; d) M. Latroche, S. Surblé, C. Serre, C. Mellot-Draznieks, P. L. Llewellyn, J.-H. Lee, J.-S. Chang, S. H. Jung, G. Férey, *Angew. Chem.* **2006**, *118*, 8407; *Angew. Chem. Int. Ed.* **2006**, *45*, 8227; e) A. G. Wong-Foy, O. Lebel, A. J. Matzger, *J. Am. Chem. Soc.* **2007**, *129*, 15740; f) F. Nouar, J. F. Eubank, T. Bousquet, L. Wojtas, M. J. Zaworotko, M. Eddaoudi, *J. Am. Chem. Soc.* **2008**, *130*, 1833.
- [2] a) G. Férey, M. Latroche, C. Serre, F. Millange, T. Loiseau, A. Percheron-Guégan, *Chem. Commun.* **2003**, 2976; b) A. G. Wong-Foy, A. J. Matzger, O. M. Yaghi, *J. Am. Chem. Soc.* **2006**, *128*, 3494; c) X. Lin, J. Jia, X. Zhao, K. M. Thomas, A. J. Blake, G. S. Walker, N. R. Champness, P. Hubberstey, M. Schröder, *Angew. Chem.* **2006**, *118*, 7518; *Angew. Chem. Int. Ed.* **2006**, *45*, 7358; d) M. Dincă, A. Dailly, Y. Liu, C. M. Brown, J. A. Neumann, J. R. Long, *J. Am. Chem. Soc.* **2006**, *128*, 16876; e) D. J. Collins, H.-C. Zhou, *J. Mater. Chem.* **2007**, *17*, 3154; f) H. Furukawa, M. A. Miller, O. M. Yaghi, *J. Mater. Chem.* **2007**, *17*, 3197; g) S. S. Kaye, A. Dailly, O. M. Yaghi, J. R. Long, *J. Am. Chem. Soc.* **2007**, *129*, 14176; h) W. Zhou, H. Wu, M. R. Hartman, T. Yildirim, *J. Phys. Chem. C* **2007**, *111*, 16131.
- [3] a) S.-H. Cho, B. Ma, S. T. Nguyen, J. T. Hupp, T. E. Albrecht-Schmitt, *Chem. Commun.* **2005**, 2563; b) C.-D. Wu, A. Hu, L. Zhang, W. Lin, *J. Am. Chem. Soc.* **2005**, *127*, 8940; c) T. K. Maji, R. Matsuda, S. Kitagawa, *Nat. Mater.* **2007**, *6*, 142; d) S. Ma, D. Sun, X.-S. Wang, H.-C. Zhou, *Angew. Chem.* **2007**, *119*, 2510; *Angew. Chem. Int. Ed.* **2007**, *46*, 2458; e) S. Hasegawa, S. Horike, R. Matsuda, S. Furukawa, K. Mochizuki, Y. Kinoshita, S. Kitagawa, *J. Am. Chem. Soc.* **2007**, *129*, 2607; f) J. Y. Lee, D. H. Olson, L. Pan, T. J. Emge, J. Li, *Adv. Funct. Mater.* **2007**, *17*, 1255; g) S. Horike, M. Dincă, K. Tamaki, J. R. Long, *J. Am. Chem. Soc.* **2008**, *130*, 5854.
- [4] a) C. Janiak, *Dalton Trans.* **2003**, 2781; b) S. Kitagawa, R. Kitaura, S.-i. Noro, *Angew. Chem.* **2004**, *116*, 2388; *Angew. Chem. Int. Ed.* **2004**, *43*, 2334; c) G. Férey, *Chem. Soc. Rev.* **2008**, *37*, 191; d) M. Dincă, J. R. Long, *Angew. Chem. Int. Ed.* **2008**, *47*, 6766.
- [5] M. Eddaoudi, D. B. Boler, H. Li, B. Chen, T. M. Reineke, M. O'Keeffe, O. M. Yaghi, *Acc. Chem. Res.* **2001**, *34*, 319.
- [6] a) C. Mellot-Draznieks, J. M. Newsam, A. M. Gorman, C. M. Freeman, G. Férey, *Angew. Chem.* **2000**, *112*, 2358; *Angew. Chem. Int. Ed.* **2000**, *39*, 2270; b) G. Férey, C. Serre, C. Mellot-Draznieks, F. Millange, S. Surblé, J. Dutour, I. Margiolaki, *Angew. Chem.* **2004**, *116*, 6456; *Angew. Chem. Int. Ed.* **2004**, *43*, 6296; c) V. A. Blatov, L. Carlucci, G. Ciani, D. M. Proserpio, *CrystEngComm* **2004**, *6*, 377; d) O. Delgado-Friedrichs, M. O'Keeffe, O. M. Yaghi, *Phys. Chem. Chem. Phys.* **2007**, *9*, 1035.
- [7] a) B. F. Hoskins, R. Robson, *J. Am. Chem. Soc.* **1990**, *112*, 1546; b) H.-C. Yeh, R.-H. Lee, L.-H. Chan, T.-Y. J. Lin, C.-T. Chen, E. Balasubramanian, Y.-T. Tao, *Chem. Mater.* **2001**, *13*, 2788.
- [8] The poor quality of the X-ray diffraction data and extreme disorder of the solvent molecules did not allow determination of whether the bound solvent molecules in **1** are DMF or water.
- [9] a) H. Li, C. E. Davis, T. L. Groy, D. G. Kelley, O. M. Yaghi, *J. Am. Chem. Soc.* **1998**, *120*, 2186; b) K. O. Kongshaug, H. Fjellvåg, *Solid State Sci.* **2003**, *5*, 303; c) J. Tao, Z.-J. Ma, R.-B. Huang, L.-S. Zheng, *Inorg. Chem.* **2004**, *43*, 6133; d) M. Dincă, J. R. Long, *J. Am. Chem. Soc.* **2005**, *127*, 9376; e) M. Dincă, A. F. Yu, J. R. Long, *J. Am. Chem. Soc.* **2006**, *128*, 8904.
- [10] K. S. Park, Z. Ni, A. P. Côté, J. Y. Choi, R. Huang, F. J. Uribe-Romo, H. K. Chae, M. O'Keeffe, O. M. Yaghi, *Proc. Natl. Acad. Sci. USA* **2006**, *103*, 10186.
- [11] a) M. Dincă, W. S. Han, Y. Liu, A. Dailly, C. M. Brown, J. R. Long, *Angew. Chem.* **2007**, *119*, 1441; *Angew. Chem. Int. Ed.* **2007**, *46*, 1419; b) M. Dincă, A. Dailly, C. Tsay, J. R. Long, *Inorg. Chem.* **2008**, *47*, 11.
- [12] a) H. Chun, D. Kim, D. N. Dybtsev, K. Kim, *Angew. Chem.* **2004**, *116*, 989; *Angew. Chem. Int. Ed.* **2004**, *43*, 971; b) S. Ma, H.-C. Zhou, *J. Am. Chem. Soc.* **2006**, *128*, 11734; c) L. Xie, S. Liu, C. Gao, R. Cao, J. Cao, C. Sun, Z. Su, *Inorg. Chem.* **2007**, *46*, 7782.
- [13] R.-Q. Zou, R.-Q. Zhong, M. Du, T. Kiyobayashi, Q. Xu, *Chem. Commun.* **2007**, 2467.
- [14] M. Dincă, J. R. Long, *J. Am. Chem. Soc.* **2007**, *129*, 11172.
- [15] a) J. Jia, X. Lin, C. Wilson, A. J. Blake, N. R. Champness, P. Hubberstey, G. Walker, E. J. Cussen, M. Schröder, *Chem. Commun.* **2007**, 840; b) H. Chun, H. Jung, G. Koo, H. Jeong, D.-K. Kim, *Inorg. Chem.* **2008**, *47*, 5355; c) X.-S. Wang, S. Ma, K. Rauch, J. M. Simmons, D. Yuan, X. Wang, T. Yildirim, W. C. Cole, J. J. López, A. de Meijere, H.-C. Zhou, *Chem. Mater.* **2008**, *20*, 3145; d) F. Nouar, J. F. Eubank, T. Bousquet, L. Wojtas, M. J. Zaworotko, M. Eddaoudi, *J. Am. Chem. Soc.* **2008**, *130*, 1833.

Received: July 2, 2008
Published online: October 9, 2008